IEEE Open Journal of
Antennas and Propagation

Received 8 September 2021; revised 23 October 2021; accepted 25 October 2021. Date of publication 1 November 2021;
date of current version 17 November 2021.

Digital Object Identifier 10.1109/OJAP.2021.3124338

Absorptive Microstrip-Fed Slot Antenna With Wide Reflectionless Band by Loading Bandstop Filter

YANQUN LIU (Member, IEEE), PENG ZHOU (Student Member, IEEE), SHUNLI LI (Member, IEEE), HONGXIN ZHAO (Member, IEEE), AND XIAOXING YIN (Member, IEEE)

State Key Laboratory of Millimeter Waves, Southeast University, Nanjing 210096, China

CORRESPONDING AUTHOR: X. YIN (e-mail: xxyin@seu.edu.cn)

This work was supported in part by the National Natural Science Foundation of China under Grant 61771127 and Grant 61801116.

ABSTRACT This paper presents an absorptive microstrip-fed slot antenna with a wide reflectionless band and high radiation efficiency. The proposed antenna consists of a microstrip-fed slot antenna, a quarter-wavelength coupled-line bandstop filter (BSF), and absorptive resistors attached to a grounding pad. The BSF and absorptive resistors are connected to the end of the microstrip feedline. The slot antenna and the BSF are designed to work at the same frequency. In the working band, the high input impedance of the BSF exactly matches the slot antenna for effective radiation. While out of the working band, since the input impedance looking towards the end of the slot antenna matches well with that of the BSF, the energy will flow through the BSF and then be absorbed by the absorptive resistors. In this way, the energy both in and out of the working band will not be reflected back to the input port, which presents a wide reflectionless band. To demonstrate this idea, a prototype operating at 3 GHz is designed, fabricated, and measured. The measurements show that the proposed antenna is well matched ($|S_{11}| < -10$ dB) in a wide frequency band from DC to 5.3 GHz, the 3-dB gain bandwidth covers from 2.85 GHz to 3.24 GHz with a peak gain of 4.54 dBi, the peak radiation efficiency can reach 93%, and a bidirectional radiation pattern is realized with more than 20 dB cross-polarization suppression in main radiation directions.

INDEX TERMS Absorptive antenna, bandstop filter, reflectionless, slot antenna.

I. INTRODUCTION

HIGHER requirements of the out-of-band performance of antennas are put forward to adapt to the current complex communication environment [1]–[4]. For most conventional reflective antennas, the spurious signals out of the working band would be inevitably reflected back to the input port, leading to the negative effects on the stability and the sensitivity of a transceiver system [5], [6]. To avoid or mitigate these problems, some complex and extra microwave devices, including isolators, circulators, diplexers, or even attenuators, are widely added to the RF front-end [5], [6]. However, this approach drastically increases the volume, cost, and insertion loss of the systems. Therefore, it is a good alternative solution to use reflectionless antennas with impedance matching both in and out of the working band.

There have been some reports about non-reflecting/reflectionless/absorptive antennas so far. In 1965, a continuous resistive profile for loading a dipole antenna to produce a pure outward-traveling wave was obtained by Wu and King [7]. This profile has been widely used in linear dipoles for short pulse applications [8]–[10]. Nevertheless, this method is hard to eliminate low-frequency reflective energy. To overcome this drawback, a matching resistor loaded at the end of a spiral slot antenna [11] was used to absorb the non-radiated incident energy, resulting in the non-reflecting feature in the entire frequency band. Similarly, a resistive absorption structure consisting of chip resistors and inductors was introduced to absorb the low-frequency energy that can not be radiated in an ultra-wideband Gaussian tapered slotline antenna [12], [13]. However, the antennas in [11]–[13] show a lower gain and radiation efficiency than original antennas without a loading structure. In the above designs, the achievements of the non-reflecting/reflectionless characteristics are at the expense of the antenna gain and

radiation efficiency. This is because the absorption effect still exists in the working band. Therefore, it is still a great challenge to achieve the non-reflecting/reflectionless characteristic out of the working band, and simultaneously maintain a high radiation efficiency in the working band.

Recently, the complementary-duplexer structure consisting of a main and an auxiliary channel with opposite filtering transfer functions is widely used in absorptive/reflectionless filter designs [14]–[18]. Inspired by this concept, a new kind of narrowband absorptive filtering patch antenna was firstly proposed in [19], where a filtering patch antenna and a defected ground structure bandstop filter are elaborately combined to realize a reflectionless characteristic. Compared to a conventional patch antenna, the modified antenna can maintain a high radiation efficiency and gain in the working band, and achieve a reflectionless characteristic within adjacent unworking bands. However, the antenna structure is relatively complex, and the reflectionless bandwidth is not very wide.

To realize broadband reflectionless characteristics out of the working band and high radiation efficiency in the working band simultaneously, a novel absorptive microstrip-fed slot antenna is proposed in this paper. Considering the structural features of a conventional microstrip-fed slot antenna, a narrowband coupled-line bandstop filter, with one port terminated by absorptive resistors, is connected to the microstrip feedline. The key point of the design is to ensure that both the slot antenna and the BSF work at the same frequency. In this way, the BSF can provide a total reflection for matching the radiating slot in the working band. Meanwhile, the incident energy out of the working band directly flows into the absorptive resistors with little coupling to the slot antenna. Thus, a reflectionless characteristic both in and out of the working band is realized. Furthermore, the prototype with a high radiation efficiency at 3 GHz, and a wide reflectionless frequency band from DC to 5.3 GHz is achieved by both simulation and measurement. Besides, the absorptive resistors are modeled as the second port in the design procedure, which greatly facilitates the design.

II. ANTENNA CONFIGURATION

Fig. 1(a) shows the geometry of the proposed absorptive microstrip-fed slot antenna on a single layer substrate. As can be seen, the proposed antenna consists of a microstrip feedline, a slot etched on the ground plane, a quarter-wavelength microstrip resonator parallel with the feedline, and two absorptive resistors attached to a grounding pad. The slot and the ground plane are located at the bottom layer of the substrate, while the feedline, the quarter-wavelength resonator, and the absorptive resistors are positioned on the top layer of the substrate. The grounding pad is connected to the ground plane through many shorting pins.

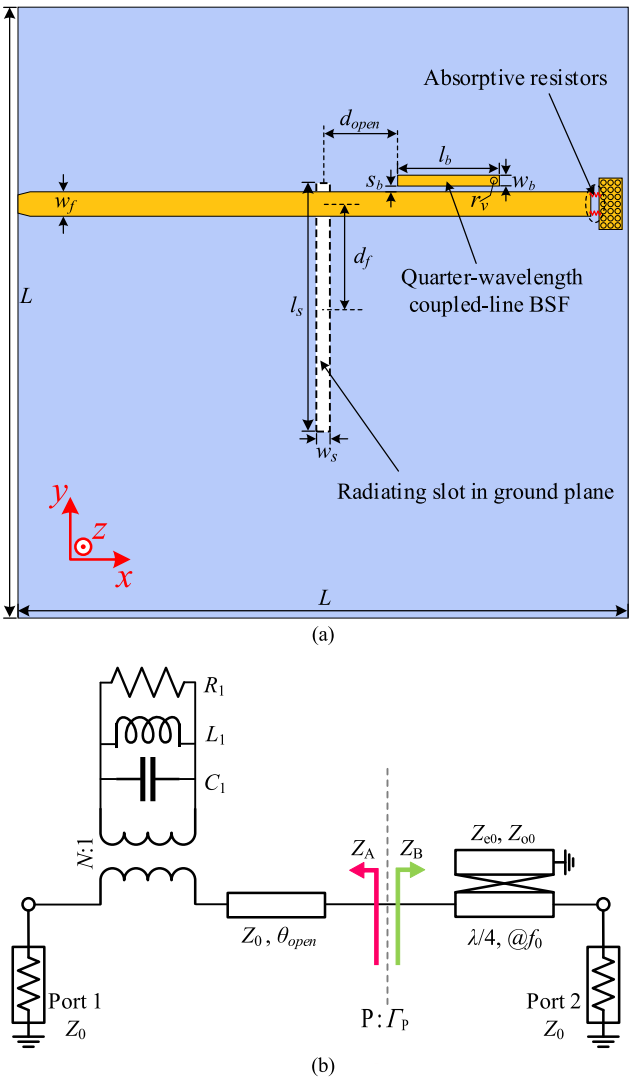

FIGURE 1. The proposed absorptive microstrip-fed slot antenna. (a) Planar structure. (b) Equivalent circuit model.

III. EQUIVALENT CIRCUIT AND ANALYSIS

A. TWO-PORT EQUIVALENT CIRCUIT OF THE PROPOSED ANTENNA

Fig. 1(b) illustrates the two-port equivalent circuit of the proposed absorptive microstrip-fed slot antenna. In this circuit model, the absorptive resistors and the grounding pad are modeled as Port 2, which will greatly facilitate the proposed design as shown in the following.

As observed, the microstrip-fed slot antenna can be modeled as a microstrip-to-slot transformer with a turn ratio of N to convert the radiation admittance ($Y_s = 1/R_1 + j\omega C_1 + 1/j\omega L_1$) into its resultant series counterpart [20]–[23], where the L_1 and C_1 resonate at the central working frequency f_0. The narrowband bandstop filter [24] is modeled as a quarter-wavelength coupled-line structure with an even-mode impedance Z_{e0} and an odd-mode impedance Z_{o0} [18], [25]. The matching line between the slot and the coupled line is

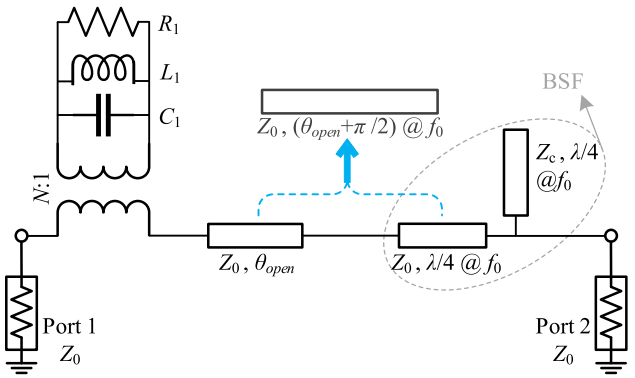

FIGURE 2. Equivalent transmission-line model of the circuit model in Fig. 1(b).

modeled as a transmission line with an electrical length of θ_{open} at f_0.

B. PRINCIPLE OF A WIDE REFLECTIONLESS BAND

According to the equivalent transmission-line model of the quarter-wavelength coupled line in [15] and [26], the equivalent transmission-line model of the proposed absorptive antenna can be obtained as in Fig. 2. For matching the slot antenna, the θ_{open} should be equal to quarter-wavelength at the working frequency f_0. In this case, these two quarter-wavelength transmission lines can be combined into one half-wavelength transmission line as also shown in Fig. 2. The corresponding ABCD-matrix between the two ports can be calculated as

$$\begin{bmatrix} A & B \\ C & D \end{bmatrix} = \frac{1}{N}\begin{bmatrix} 1 & \frac{1}{\frac{1}{R_1}+j\omega C_1+\frac{1}{j\omega L_1}} \\ 0 & N^2 \end{bmatrix} \cdot \begin{bmatrix} \cos\left(\beta\frac{\lambda_0}{2}\right) & jZ_0\sin\left(\beta\frac{\lambda_0}{2}\right) \\ \frac{j\sin\left(\beta\frac{\lambda_0}{2}\right)}{Z_0} & \cos\left(\beta\frac{\lambda_0}{2}\right) \end{bmatrix} \times \begin{bmatrix} 1 & 0 \\ j\frac{1}{Z_c}\tan\left(\beta\frac{\lambda_0}{4}\right) & 1 \end{bmatrix}. \quad (1)$$

Based on the narrowband filter synthesis theory, the element values of the L_1 [26], C_1 [26], and Z_c [15] can be extracted according to

$$C_1 = g_1/\eta_A\omega_0 Z_0 \quad (2)$$

$$L_1 = 1/\omega_0^2 C_1 \quad (3)$$

$$Z_c = 4Z_0/\pi\eta_B g_0 g_1 \quad (4)$$

where the η_A and η_B are respectively the fractional bandwidth of the slot antenna and the BSF, and the g_0 and g_1 are the element values of the one-order Chebyshev low-pass prototype.

Substituting (2)-(4) into (1) yields

$$\begin{bmatrix} A & B \\ C & D \end{bmatrix} = \frac{1}{N}\begin{bmatrix} 1 & \frac{1}{\frac{1}{R_1}+j\frac{g_1}{\eta_A Z_0}\left(\Omega-\frac{1}{\Omega}\right)} \\ 0 & N^2 \end{bmatrix} \cdot \begin{bmatrix} \cos(\pi\Omega) & jZ_0\sin(\pi\Omega) \\ \frac{j\sin(\pi\Omega)}{Z_0} & \cos(\pi\Omega) \end{bmatrix} \times \begin{bmatrix} 1 & 0 \\ j\frac{\pi\eta_B g_0 g_1}{4Z_0}\tan\left(\frac{\pi}{2}\Omega\right) & 1 \end{bmatrix} \quad (5)$$

where the $\Omega = \omega/\omega_0$.

According to the above ABCD-matrix, the frequency responses of the circuit model can be obtained. To simplify the analysis, a typical value of the turn ratio $N = 1$ is selected, and the radiation resistor $R_1 = 50$ ohms is used. When the reference return loss is set as 10 dB in the synthesis process, the $g_0 = 1$ and $g_1 = 0.68$ can be obtained [26]. The reference impedance Z_0 is equal to 50 ohms.

Since the thin slot antenna is narrowband, the antenna bandwidth η_A is set as 0.1 here. The effects of η_B on the frequency responses of the equivalent circuit model are shown in Fig. 3. As can be seen, with the BSF bandwidth η_B increasing, the reflection coefficient drastically deteriorates across the whole frequency band, especially near the working band. This is because the energy reflected by the BSF can not be totally radiated by the slot antenna when the BSF bandwidth is too large.

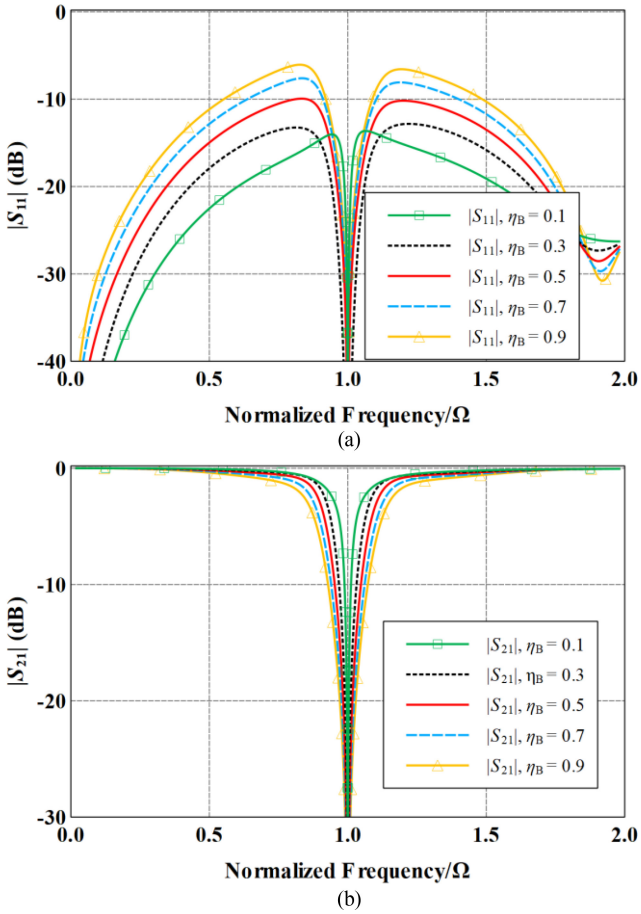

FIGURE 3. Effect of the η_B on the responses of the equivalent circuit model. (a) $|S_{11}|$. (b) $|S_{21}|$. ($\eta_A = 0.1$).

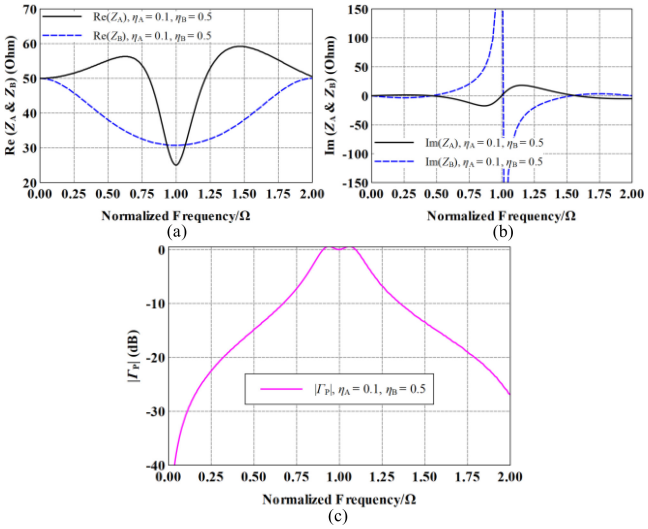

FIGURE 4. (a) Real parts and (b) Imaginary parts of the impedance of Z_A and Z_B. (c) $|\Gamma_P|$ at circuit node P.

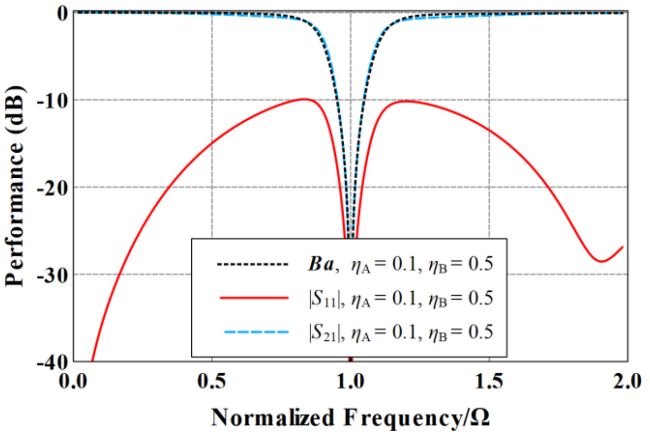

FIGURE 5. $|S_{11}|$, $|S_{21}|$ and *Ba* of the two-port equivalent circuit model ($\eta_A = 0.1$, $\eta_B = 0.5$).

To explain the principle of a wide reflectionless band in detail, the transmission characteristic at circuit node P is studied. As shown in Fig. 1(b), the Z_A and Z_B are the input impedance respectively looking into the antenna and the BSF. In the case of $\eta_A = 0.1$ and $\eta_B = 0.5$, the real and imaginary parts of Z_A and Z_B are respectively shown in Fig. 4(a) and (b). As can be seen, serious impedance mismatch mainly occurs in the frequency band around the center working frequency. While in the lower and higher frequency band, both the real and imaginary parts of the Z_A and Z_B have a good match. For a more intuitive presentation, the reflection coefficient at circuit node P is shown in Fig. 4(c), where the $\Gamma_P = |(Z_B - Z_A)/(Z_B + Z_A)|$. According to the reflection coefficient Γ_P, we can infer that the energy in the lower and higher frequency band will flow through the BSF and then be absorbed by Port 2. As for the energy near the center frequency, most of it will be reflected by the BSF and then be radiated by the slot antenna. This is because the high resistance of Z_B exactly matches the slot antenna for efficient radiation in the working band. In this way, the energy both in and out of the working band will not be reflected back to the input port, which presents a wide reflectionless band.

C. EFFECTIVE RADIATION BANDWIDTH OF THE PROPOSED DESIGN

The responses of the equivalent transmission-line model in Fig. 2 with $\eta_A = 0.1$ and $\eta_B = 0.5$ are presented in Fig. 5. Herein, a parameter named ***Ba*** is defined as

$$\boldsymbol{Ba} = |S_{11}|^2 + |S_{21}|^2. \tag{6}$$

As in (6), (1-***Ba***) presents the power dissipated in the radiation resistor R_1. Therefore, the ***Ba*** can be used to characterize the effective radiation bandwidth of the proposed design. Moreover, the ***Ba*** and $|S_{21}|$ are also compared in Fig. 5. As can be seen, the ***Ba*** is well matched with the $|S_{21}|$, which means the effective radiation bandwidth mainly depends on the $|S_{21}|$ of the two-port model. And the bandwidth of the $|S_{21}|$ is determined by that of the BSF as shown in Fig. 3(b).

According to the above analysis of the equivalent circuit model, when the bandwidth of the slot antenna is determined, a better reflectionless characteristic requires a narrower bandwidth of the loaded BSF, but a wider effective radiation bandwidth requires a wider bandwidth of the loaded BSF. Therefore, in the design of the proposed absorptive slot antenna, it is necessary to make a compromise between the reflectionless characteristic and effective radiation bandwidth, which can be realized by selecting a suitable bandwidth of the loaded BSF.

IV. ANTENNA IMPLEMENTATION

The proposed antenna is designed on the Rogers RO4003C substrate, which has a dielectric constant of 3.55 and a loss tangent of 0.0027. The thickness of the substrate in this design is 1.524 mm.

The design of the proposed absorptive slot antenna starts from the study of a conventional microstrip-fed slot antenna, and then a BSF and absorptive resistors are integrated with the slot antenna.

A. HARMONIC SUPPRESSION OF CONVENTIONAL MICROSTRIP-FED SLOT ANTENNA

In our design, the slot antenna works at the half-wavelength resonant mode, and the length of the slot can be calculated according to

$$l_s = c/2f_0\sqrt{\varepsilon_e} \tag{7}$$

where ε_e is the effective dielectric constant of the slot line [27], f_0 is the resonant frequency of the slot, and c is the speed of light in free space. As in [21], the bandwidth of a microstrip-fed slot antenna mainly depends on the width of the slot. Herein, a 10% FBW at 3 GHz is chosen for a narrowband verification of the proposed design. In

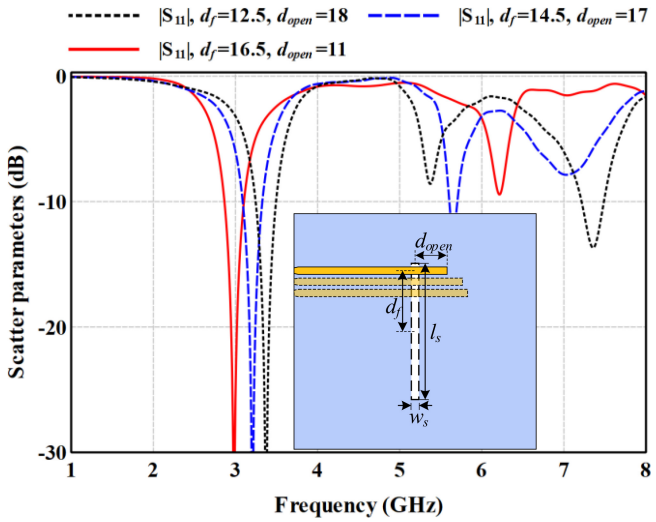

FIGURE 6. Parameter investigation of a conventional microstrip-fed slot antenna, where the $l_S = 36.5$ mm and $w_S = 2$ mm.

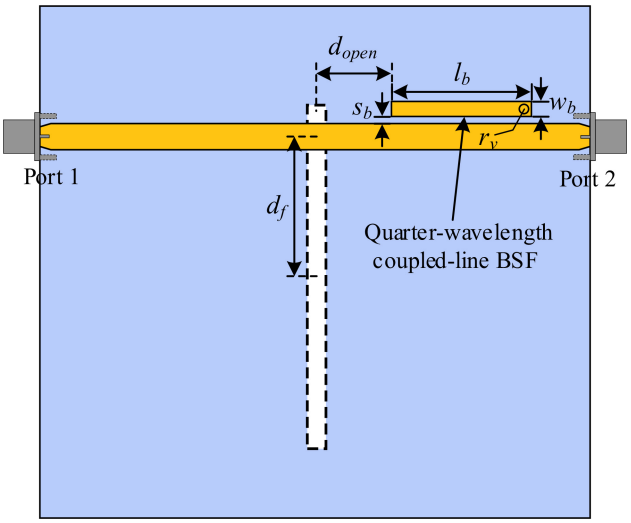

FIGURE 7. Integration of the slot antenna and the BSF, where the $l_b = 15$ mm, $w_b = 1.2$ mm, $s_b = 0.3$ mm, and $r_v = 0.3$ mm.

this case, the slot with a length of 36.5 mm and a width of 2 mm is initially determined by a full-wave simulation in commercial simulation software CST.

As in [26], the resonant modes of the defected ground structure in a planar transmission line would give rise to the bandstop characteristic. Similarly, the higher-order harmonic of the slot antenna will lead to a strong reflection in our design. Therefore, a wider frequency spacing between the working mode and harmonic is conducive to achieving a wider reflectionless frequency band. Parameter investigations in Fig. 6 indicate that the feeding position significantly affects the harmonic characteristic of a conventional microstrip-fed slot antenna. As can be seen, with the feeding position shifting to the end of the slot, the higher-order modes move to a higher frequency, which leads to a good harmonic suppression characteristic. Besides, with the movement of the feeding point, the working frequency of the slot antenna has a slight shift, and the length of the feedline beyond the slot should also be adjusted for matching the radiating slot working at the designed frequency 3 GHz.

B. INTEGRATION WITH THE BSF AND ABSORPTIVE RESISTORS

According to the equivalent circuit model in Fig. 1(b), a two-port prototype of the proposed absorptive microstrip-fed slot antenna is presented in Fig. 7. As can be seen, a narrowband BSF with a quarter-wavelength coupled-line structure is connected after the feedline, and then with Port 2 terminated.

As the previous analysis, the BSF is also designed at 3 GHz with an initial FBW of about 50%, and the initial element values of the coupled-line structure can be determined by a full-wave simulation in CST, listing as $l_b = 14.8$ mm, $w_b = 1.2$ mm, $s_b = 0.2$ mm, and $r_v = 0.3$ mm.

As depicted in Fig. 7, the distance (d_{open}) between the slot and the quarter-wavelength resonator affects the matching status of the radiating slot, and the gap between the coupled line (s_b) determines the bandwidth of the BSF. As in Fig. 8(a), a longer or shorter length of the matching line would deteriorate the impedance matching near the working frequency band. The sensitivity analysis about s_b is presented in Fig. 8(b). It can be found that the changing trend is similar to those in Fig. 3, which further confirms the effectiveness of the circuit model in Figs. 1 and 2. Moreover, there is a maximum point of the reflection coefficient around 6 GHz, this is caused by the excitation of the higher-order mode of the slot on the ground plane as shown in Fig. 6. Changing the feeding position of the radiating slot can alleviate this phenomenon as shown in Figs. 6 and 8(c). That is why the feeding position of the proposed design is close to the end of the slot.

After the design of the two-port model is completed, two resistors and a grounding pad are attached to the end of the feedline to replace Port 2, as shown in Fig. 1. Because the feedline is relatively wide, two resistors with 100 Ω are parallelly placed on the two sides of the feedline, which ensures a better absorption characteristic, especially in higher frequency. The pad with many shorting pins can provide a good grounding effect.

Besides, the current distributions in and outside the working band are depicted in Fig. 9, which is an intuitive representation of the working mechanism of the proposed antenna. As can be seen, in the working band (at 3 GHz), the incident power is strongly coupled to the radiating slot and the quarter-wavelength resonator, and almost no power flows into the absorptive resistors. While outside the working band (at 4 GHz), the incident power directly flows into the absorptive resistors with little coupling with the slot and the quarter-wavelength resonator.

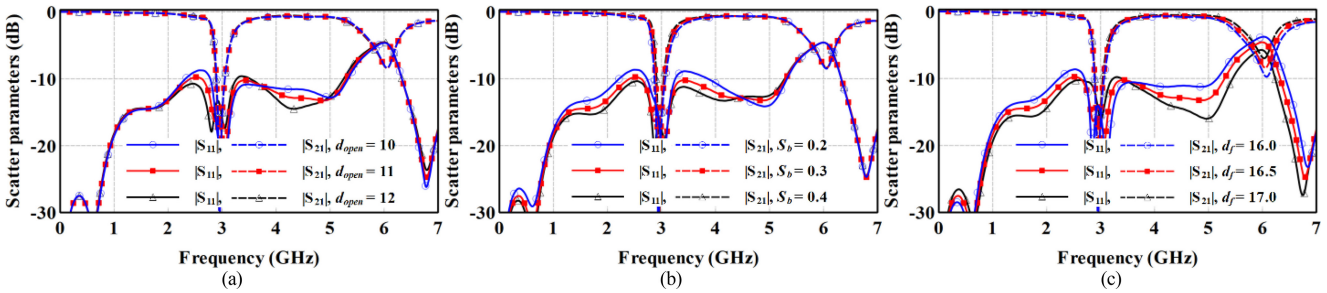

FIGURE 8. Parameter investigations of the two-port prototype.

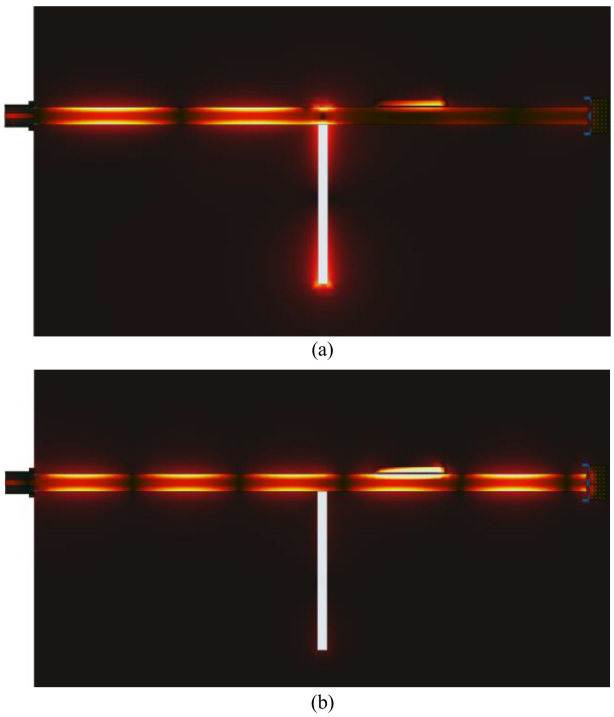

FIGURE 9. Current distributions of the proposed antenna. (a) 3 GHz (In-Band). (b) 4 GHz (Out-of-Band).

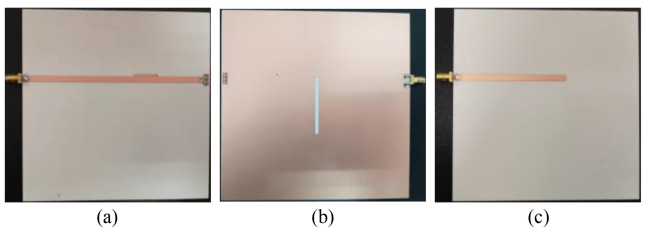

FIGURE 10. Fabricated prototypes. (a) Top view, (b) Bottom view of proposed absorptive slot antenna. (c) Top view of a conventional microstrip-fed slot antenna.

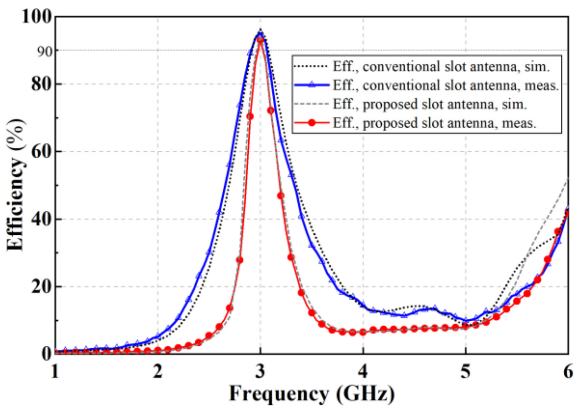

FIGURE 11. The simulated and measured antenna efficiencies of the proposed absorptive slot antenna and the conventional microstrip-fed slot antenna.

V. MEASUREMENT AND DISCUSSION

To verify the proposed design, a prototype working at 3.0 GHz is optimized and fabricated. The fabricated antenna parameters are as follows: $L = 120$ mm, $w_f = 3.6$ mm, $l_s = 36.4$ mm, $w_s = 2.0$ mm, $d_f = 16.7$ mm, $d_{open} = 10.7$ mm, $l_b = 15$ mm, $w_b = 1.2$ mm, $s_b = 0.3$ mm, and $r_v = 0.3$ mm. The absorptive resistors are Panasonic's chip resistor with a 0402 package, and the resistance value is 100 Ω. The reflection coefficient is measured by a Keysight PNA Network Analyzer N5224A, and the radiation patterns, radiation efficiency, and antenna gains are measured by a Satimo near-field measure system in Nanjing University of Posts and Telecommunications, Nanjing, China.

For comparison, a conventional microstrip-fed slot antenna is also fabricated, and the two fabricated prototypes are shown in Fig. 10. As depicted, the proposed absorptive slot antenna maintains the original structure of a conventional microstrip-fed slot antenna, except for the introduced quarter-wavelength resonator, absorptive resistors, and grounding pad.

The simulated and measured antenna efficiencies of the two fabricated prototypes are shown in Fig. 11. As observed, the measured and simulated antenna efficiencies are in good agreement, and the measured peak radiation efficiency of the proposed absorptive design in the working band is up to 93%, comparable to the conventional microstrip-fed slot antenna.

The simulated and measured reflection coefficients and antenna gains of the two prototypes are shown in Fig. 12. As can be seen, different from a conventional reflective slot antenna, the proposed absorptive slot antenna shows a wide reflectionless frequency band from DC to 5.3 GHz, and an absorptive characteristic even in the higher frequency band is also obtained. The deviation between the measured and simulated reflection coefficients of the proposed absorptive slot antenna mainly comes from the non-ideality of the absorptive

TABLE 1. Comparison with previous works.

	Loading method	Quasi-reflectionless band ($\|S_{11}\|$< -10 dB)	3dB gain bandwidth/ Peak gain	Peak radiation efficiency	Antenna type
[11]	single resistor loading	DC~8 GHz	ultra-wideband/ N.A.	21%	spiral slot antenna
[13]	single resistor and single inductor loading	DC~10 GHz	ultra-wideband/ 8.79 dBi @ 9 GHz	63%	tapered slot antenna
[19]	BSF and absorptive resistor loading	5~6.5 GHz (0.86~1.12 f_0)	5.56~6.06 GHz/ 7.28 dBi @ 5.8 GHz	78%	patch antenna
This work	**BSF and absorptive resistors loading**	**DC~5.3 GHz (0~1.76 f_0)**	**2.85~3.24 GHz/ 4.54 dBi @ 3 GHz**	**93%**	**slot antenna**

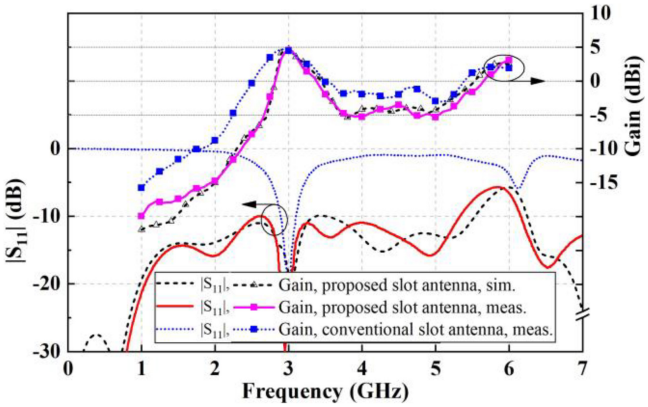

FIGURE 12. $|S_{11}|$ and gains of the proposed absorptive slot antenna and the conventional microstrip-fed slot antenna.

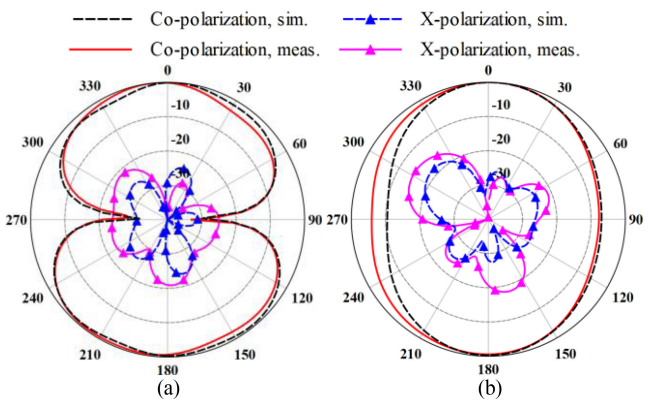

FIGURE 13. Normalized radiation patterns of the proposed antenna at 3 GHz. (a) E-plane. (b) H-plane.

resistors. The measured 3-dB gain bandwidth is from 2.85 GHz to 3.24 GHz with a peak gain of 4.54 dBi, which is consistent with the simulated ones. However, the proposed absorptive slot antenna shows a narrower gain bandwidth compared with the conventional microstrip-fed slot antenna, due to a narrower bandwidth of the $|S_{21}|$ of the loaded BSF.

Besides, the simulated and measured normalized radiation patterns are presented in Fig. 13, which shows a bidirectional radiation with more than 20 dB cross-polarization suppression in the main radiation directions.

Compared with previous reflectionless/absorptive antenna designs in Table 1, the proposed absorptive microstrip-fed slot antenna not only achieves a wide reflectionless band, but also has a high radiation efficiency in the working band. As for other existing non-reflecting/reflectionless/absorptive antennas [11], [13], [19], due to the poor frequency selectivity of the loaded absorption structure or the defects of the antenna structure, a certain amount of in-band energy also flows into the absorptive resistors, resulting in the deterioration of the radiation efficiency.

VI. CONCLUSION

In this paper, a microstrip-fed slot antenna with absorption characteristics is firstly proposed to achieve a wide reflectionless band and high radiation efficiency simultaneously. A two-port circuit model is established, which greatly facilitates the proposed design. Different from the existing absorptive/reflectionless antenna designs, the proposed design is more like a narrowband loading technique than a combination of an antenna and a BSF. Therefore, our design maintains the original structure and radiation characteristics of a conventional microstrip-fed slot antenna. Furthermore, this absorptive antenna design based on the BSF-loaded method can be easily extended to many kinds of antennas with similar feeding arrangements. The use of absorptive/reflectionless antennas can alleviate the problems caused by the reflected signal noise at the transmitter front-end, and has significant theoretical and application value.

ACKNOWLEDGMENT

The authors would like to thank Prof. D. Chen and W.-J. Lu from the Nanjing University of Posts and Telecommunications, Nanjing, China, for their beneficial discussion on antenna design and measurement.

REFERENCES

[1] R. Garg, P. Bhartia, I. Bahl, and A. Ittipiboon, *Microstrip Antenna Design Handbook*. Norwood, MA, USA: Artech House, 2001.
[2] R. Waterhouse, *Printed Antennas for Wireless Communications*. Hoboken, NJ, USA: Wiley, 2007.
[3] E. H. Lim and K. W. Leung, *Compact Multifunctional Antennas for Wireless Systems*. Hoboken, NJ, USA: Wiley, 2012.
[4] K. Chang, R. York, P. Hall, and T. Itoh, "Active integrated antennas," *IEEE Trans. Microw. Theory Techn.*, vol. 50, no. 3, pp. 937–944, Mar. 2002.
[5] Q. Gu, *RF System Design of Transceivers for Wireless Communications*. New York, NY, USA: Springer, 2005.
[6] G. Hueber and R. B. Staszewski, *Multi-Mode/Multi-Band RF Transceivers for Wireless Communications: Advanced Techniques Architectures and Trends*. New York, NY, USA: Wiley, 2011.

[7] T. Wu and R. King, "The cylindrical antenna with nonreflecting resistive loading," *IEEE Trans. Antennas Propag.*, vol. 13, no. 3, pp. 369–373, May 1965.
[8] L.-C. Shen, "An experimental study of the antenna with nonreflecting resistive loading," *IEEE Trans. Antennas Propag.*, vol. 15, no. 5, pp. 606–611, Sep. 1967.
[9] Y.-P. Liu and D. Sengupta, "Transient radiation from a linear antenna with nonreflecting resistive loading," *IEEE Trans. Antennas Propag.*, vol. 22, no. 2, pp. 212–220, Mar. 1974.
[10] W. Kang, K. Kim, and W. Kim, "A broad-band conductively-loaded slot antenna for pulse radiation," *IEEE Trans. Antennas Propag.*, vol. 62, no. 1, pp. 33–39, Jan. 2014.
[11] M. Yang, Y. Li, X. Yin, and X. Wang, "Ultra-wideband non-reflecting planar spiral slot antenna using post-wall structure," in *Proc. 6th Asia–Pacific Conf. Antennas Propag. (APCAP)*, Xi'an, China, 2017, pp. 1–3.
[12] H. Chen, Q. Zhang, J. Gao, S. Li, H. Zhao, and X. Yin, "Ultra-wideband reflectionless tapered slotline antenna with resistive absorption structure," in *Proc. Int. Symp. Antennas Propag. (ISAP)*, Xi'an, China, 2019, pp. 1–3.
[13] S. Li, H. Chen, Q. Zhang, M. Yang, H. Zhao, and X. Yin, "Time-domain analysis and design of pulse matching tapered slotline antenna with resistive and reactive loading network," *IEEE Trans. Antennas Propag.*, vol. 69, no. 7, pp. 3689–3699, Jul. 2021.
[14] M. A. Morgan and T. A. Boyd, "Theoretical and experimental study of a new class of reflectionless filter," *IEEE Trans. Microw. Theory Techn.*, vol. 59, no. 5, pp. 1214–1221, May 2011.
[15] J.-Y. Shao and Y.-S. Lin, "Narrowband coupled-line bandstop filter with absorptive stopband," *IEEE Trans. Microw. Theory Techn.*, vol. 63, no. 10, pp. 3469–3478, Oct. 2015.
[16] D. Psychogiou and R. Gómez-García, "Reflectionless adaptive RF filters: Bandpass, bandstop, and cascade designs," *IEEE Trans. Microw. Theory Techn.*, vol. 65, no. 11, pp. 4593–4605, Nov. 2017.
[17] M. A. Morgan, "Think outside the band: Design and miniaturization of absorptive filters," *IEEE Microw. Mag.*, vol. 19, no. 7, pp. 54–62, Nov./Dec. 2018.
[18] X. Wu, Y. Li, and X. Liu, "High-order dual-port quasi-absorptive microstrip coupled-line bandpass filters," *IEEE Trans. Microw. Theory Techn.*, vol. 68, no. 4, pp. 1462–1475, Apr. 2020.
[19] Y.-T. Liu, K. W. Leung, and N. Yang, "Compact absorptive filtering patch antenna," *IEEE Trans. Antennas Propag.*, vol. 68, no. 2, pp. 633–642, Feb. 2020.
[20] Y. Yoshimura, "A microstrip slot antenna," *IEEE Trans. Microw. Theory Techn.*, vol. MTT-20, no. 11, pp. 760–762, Nov. 1972.
[21] B. N. Das and K. K. Joshi, "Impedance of a radiating slot in the ground plane of a microstripline," *IEEE Trans. Antennas Propag.*, vol. AP-30, no. 5, pp. 922–926, Sep. 1982.
[22] L. Zhu and K. Wu, "Complete circuit model of microstrip-fed slot radiator: Theory and experiments," *IEEE Microw. Guided Wave Lett.*, vol. 9, no. 8, pp. 305–307, Aug. 1999.
[23] L. Zhu, R. Fu, and K.-L. Wu, "A novel broadband microstrip-fed wide slot antenna with double rejection zeros," *IEEE Antenna Wireless Propag. Lett.*, vol. 2, pp. 194–196, 2003.
[24] H. C. Bell, "L-resonator bandstop filters," *IEEE Trans. Microw. Theory Techn.*, vol. 44, no. 12, pp. 2669–2672, Dec. 1996.
[25] D. M. Pozar, *Microwave Engineering*. Hoboken, NJ, USA: Wiley, 2012.
[26] J.-S. Hong and M. J. Lancaster, *Microwave Filters for RF/Microwave Applications*, 2nd ed. New York, NY, USA: Wiley, 2011.
[27] K. C. Gupta, R. Garg, I. Bahl, and P. Bhartia, *Microstrip Lines and Slotlines*, 2nd ed. Norwood, MA, USA: Artech House, 1996.

YANQUN LIU (Member, IEEE) was born in Kaifeng, Henan, China, in 1991. He received the B.Eng. degree in information engineering and the Ph.D. degree in electromagnetic field and microwave technology from the School of Information Science and Engineering, Southeast University, Nanjing, China, in 2014 and 2021, respectively.

His current research interests include RF circuit and system, microwave passive component, integrated design of filter and antenna, and characteristic mode analysis.

PENG ZHOU (Student Member, IEEE) was born in Nantong, Jiangsu, China, in 1995. He received the B.Sc. degree in applied physics and the M.S. degree in circuit and system from Nanjing Normal University, Nanjing, China, in 2016 and 2019, respectively. He is currently pursuing the Ph.D. degree in electromagnetic field and microwave technique with Southeast University, Nanjing. His current research interests include microwave passive devices, antenna designs, and the analysis of signal integrity in high-speed digital circuits and systems.

SHUNLI LI (Member, IEEE) was born in Liaocheng, Shandong, China, in 1984. He received the B.S. degree in science and technology of electronic information and the M.S. degree in radio physics from Shandong University in 2007 and 2010, respectively, and the Ph.D. degree in electromagnetic field and microwave technology from the State Key Laboratory of Millimeter Waves, Southeast University in 2015. In 2015, he joined the Department of Electrical and Computer Engineering, National University of Singapore, as a Research Fellow. Since 2017, he has been a Lecturer with the State Key Laboratory of Millimeter Waves, Southeast University, where he is currently an Associate Professor. His current research interests include ultrawideband antennas and systems, time-domain analysis, microwave passive devices, and short-pulse antennas and networks.

HONGXIN ZHAO (Member, IEEE) was born in Hongze, Jiangsu, China, in 1971. He received the B.Sc. degree in radio communication techniques and the Ph.D. degree in microwave techniques from Southeast University, Nanjing, China, in 1993 and 2003, respectively. In 1996, he joined the Research Team, State Key Laboratory of Millimeter Waves, Southeast University, with interest in microwave circuit design. He is interested in the research of signal processing and control.

XIAOXING YIN (Member, IEEE) was born in Taiyuan, China. He received the B.Sc. degree in radio engineering and the M.Sc. and Ph.D. degrees in electrical engineering from the Nanjing Institute of Technology (currently Southeast University), Nanjing, China, in 1983, 1989, and 2001, respectively. From 1983 to 1986 and from 1989 to 1998, he was with the Department of Physics, University of Petroleum, Dongying, China, where he was involved in logging methods and instruments. Since 2001, he has been a Lecturer with the State Key Laboratory of Millimeter Waves, Southeast University, where he is currently a Professor. He has authored or coauthored 63 technical papers. He holds over 30 patents. His current research interests include computational electromagnetics, microwave components and system, and antennas.